
INDUCED OPTICAL BISTABILITY IN SMALL METAL AND METAL COATED PARTICLES WITH NONLINEAR DIELECTRIC FUNCTIONS

O.A. BURYI,¹ L.G. GRECHKO,² V.N. MAL'NEV,³ S. SHEWAMARE³

¹Taras Shevchenko National University of Kyiv

(2, Prosp. Academician Glushkov, Kyiv 03022, Ukraine; e-mail: obur2@ukr.net)

²Institute of Surface Chemistry, Nat. Acad. of Sci. of Ukraine

(17, General Naumov Str., Kyiv-164 03680, Ukraine; e-mail: user@surfchem.freenet.kiev.ua)

³Addis Ababa University, Physics Department

(Addis Ababa, POB 1176, Ethiopia; e-mail: vnmalnev@phys.aau.edu.et)

PACS 42.65.Pc, 42.65.An,

81.05.Rm

©2011

The theoretical and numerical study of the enhancement of the amplitude of the incident electromagnetic radiation in small metal ellipsoidal particles and spherical dielectric particles covered by a metal shell with nonlinear dielectric functions is carried out. If the frequency of the external radiation approaches the frequency of surface plasmons of a metal, the local field in the particle considerably increases. At intense incident electromagnetic fields (laser radiation), it is necessary to consider the nonlinear part of the dielectric functions of a metal and a dielectric. This results in the induced optical bistability (IOB) when one value of the amplitude of the incident field initiates three values of the local field in a particle. The domains of IOB are specified in the case where the radiation wavelength is much larger than the typical size of particles. The range of external fields and the IOB frequency are specified. A decrease of the IOB domain and an increase of the critical fields with increase in the damping of plasmon vibrations are discussed. The results of numerical computations for typical small silver particles are presented graphically.

1. Introduction

The induced optical bistability (IOB) means that some nonlinear optical systems can produce two different output intensities for a given input intensity [1] or, in particular, the given value of an external electric field may produce several values for the local field and the polarization. Since its theoretical prediction in 1969 [2] and the experimental realization in 1976 [3], this effect has been intensively studied because of its potential use for

optical switching devices and in optical computing [4–12]. Recently, it has received a new attention because of the intensive study of properties of composite media and nonlinear photonic crystals [13–15].

It is clear that the nonlinear part of the dielectric function (DF) is important only if the electric fields are comparable with the inner atomic fields. At present, such fields may be achieved in laser radiation. Another interesting property of a pure metal and metal-covered dielectric small particles is the abnormal enhancement of the local field, when the frequency of the incident electromagnetic wave approaches the surface plasmon frequency of the metal. As a result, the IOB emerges at comparatively low electric fields.

The aim of this study is a detailed theoretical and numerical analysis of the local field enhancement and the bistability domain in small metal and semiconductor particles in the electrostatic approximation. We account for a cubic nonlinearity in the polarization with respect to the local electric field. In Section 1, we analyze the local field enhancement inside an ellipsoidal metal particle embedded into a dielectric matrix when the incident electric field is parallel to one of the ellipsoid axes. Section 2 is devoted to the analysis of the IOB domain for these particles. Lastly in Section 3, we study the IOB of a two-layer nonlinear dielectric spherical particle covered by a metal shell.

We also propose a comparatively simple analysis of roots for a cubic equation that may be useful for the

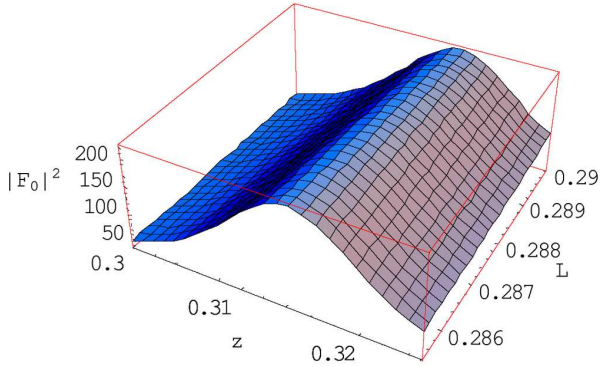


Fig. 1. Enhancement factor $|F_0|^2$ for a small silver particle versus z and L ; $\varepsilon'_h = 2.25$, $\varepsilon''_h = 0$, $\varepsilon'_\infty = 4.5$, $\varepsilon''_\infty = 0.16$, $\omega_p = 1.46 \times 10^{16}$, $\nu = 1.68 \times 10^{14}$, $\gamma = 1.15 \times 10^{-2}$

study of instability domains in the processes that are described by an S-type characteristic curve (the local field in the particle versus the applied field).

2. Enhancement of the Local Field in Small Metal Ellipsoidal Particles

Let an electromagnetic wave impinge on a metal particle in the form of a rotational ellipsoid embedded in a dielectric host matrix. The dielectric function of the particle is assumed to depend on the frequency ω and the local electric field \mathbf{E} (inside the particle) and can be presented in the form

$$\varepsilon(\omega, \mathbf{E}) = \varepsilon(\omega) + \chi(\omega) |\mathbf{E}|^2, \quad (1)$$

where $\chi(\omega)$ is the complex Kerr coefficient, $\varepsilon(\omega) = \varepsilon'(\omega) + i\varepsilon''(\omega)$ is the linear part of DF (with respect to \mathbf{E}) and taken in the Drude form

$$\varepsilon'(\omega) = \varepsilon'_\infty - \frac{\omega_p^2}{\omega^2 + \nu^2}, \quad \varepsilon''(\omega) = \varepsilon''_\infty + \frac{\nu}{\omega} \frac{\omega_p^2}{\omega^2 + \nu^2}. \quad (2)$$

Here, ω_p is the plasma frequency of electrons in the metal, ν is their collision frequency, and ε_∞ is a constant that can be a function of the frequency and depends on the type of a metal.

Let the electric vector of the incident wave \mathbf{E}_h be parallel to the large semiaxis of the ellipsoid. It is known [9] that, in the electrostatic approximation (when the wavelength of electromagnetic radiation is much larger than a typical size of the particle), the local field \mathbf{E} is uniform and parallel to \mathbf{E}_h for an arbitrary dependence of $\varepsilon(\omega, \mathbf{E})$. This electric field can be expressed in the form

$$\mathbf{E} = F \cdot \mathbf{E}_h, \quad F = \frac{\varepsilon_h}{\varepsilon_h(1-L) + L\varepsilon(\omega, \mathbf{E})}, \quad (3)$$

where F is an enhancement factor, L is a depolarization factor along the field direction which coincides in our case with the larger semiaxis of the ellipsoid, and ε_h is the dielectric function of the matrix [9]. Combining (3) and (1), we obtain the following expression for the enhancement factor:

$$F = \frac{\varepsilon_h}{L} \cdot \frac{1}{\tilde{\varepsilon}' + \chi' |\mathbf{E}|^2 + i(\tilde{\varepsilon}'' + \chi'' |\mathbf{E}|^2)}. \quad (4)$$

Here, $\tilde{\varepsilon}'$ and $\tilde{\varepsilon}''$ are the real and imaginary parts of the combination

$$\tilde{\varepsilon} \equiv \frac{\varepsilon_h(1-L) + L\varepsilon(\omega)}{L}, \quad (5)$$

and χ' and χ'' are the real and imaginary parts of $\chi(\omega)$.

We now consider the case of small electric fields such that the nonlinear term of DF (1) may be ignored. In this case, relation (4) with account of definitions (2) and (5) transforms into the expression

$$|F_0|^2 = \left| \frac{\varepsilon_h}{L} \right|^2 \frac{1}{\left(\frac{1}{z_s^2} - \frac{1}{z^2 + \gamma^2} \right)^2 + \left(\frac{1}{\bar{z}_s^2} + \frac{\gamma}{z(z^2 + \gamma^2)} \right)^2}. \quad (6)$$

Here, F_0 stands for the enhancement factor (4), where the terms with the electric field are neglected. We have also introduced the dimensionless frequencies

$$z = \frac{\omega}{\omega_p}, \quad \gamma = \frac{\nu}{\omega_p}, \quad z_s = \frac{\omega_s}{\omega_p}, \quad \bar{z}_s = \frac{\bar{\omega}_s}{\omega_p}, \quad (7)$$

$$\omega_s = \omega_p \sqrt{\frac{L}{\varepsilon'_h(1-L) + \varepsilon'_\infty L}},$$

$$\bar{\omega}_s = \omega_p \sqrt{\frac{L}{\varepsilon''_h(1-L) + \varepsilon''_\infty L}}.$$

It is important to obtain the largest values of $|F_0|^2$. It is clear that this happens if the first term in the denominator (6) is close to zero. Because of the multiparametrical dependence of $|F_0|^2$, we decided to use its 3D representation versus z and L . Figure 1 presents such a graph in the range of parameters, where $|F_0|^2$ is the largest.

One can see that the enhancement factor has a rather sharp maximum when the frequency ω approaches the frequency of the surface plasmon ω_s (7) if $\gamma \ll z$. To clarify the dependence on L , we present $|F_0|^2$ as a function of z at different constants L (Fig. 2). Inspecting

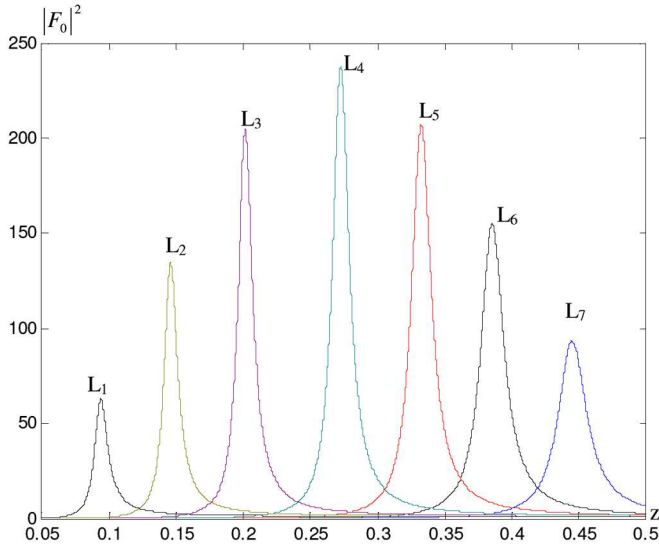


Fig. 2. Enhancement factor $|F_0|^2$ (6) as a function of the dimensionless frequency z at different L ($L_1 = 0.02$, $L_2 = 0.05$, $L_3 = 0.1$, $L_4 = 0.2$, $L_5 = 0.33$, $L_6 = 0.5$, $L_7 = 0.8$) with the same parameters of the particle and ε_h as in Fig. 1

graphs in Figs. 1 and 2, one can see that the enhancement factor $|F_0|^2$ in the physically interesting range of parameters sharply depends on the frequency of an incident electromagnetic wave ω and weakly depends on the depolarization factor decreasing with L . It can easily be seen from (6) that $|F_0|^2 = 1$ at $L \rightarrow 0$. The maximum value of $|F_0|^2$ at the accepted parameters of the particle and the host matrix is around 200. By changing ε_h and L , one can obtain even larger $|F_0|^2$. This means that, at comparatively large applied fields E_h in a vicinity of the corresponding plasma resonance, it is necessary to consider the nonlinear terms in the dielectric function (1). This will be done in the next section.

3. Bistability in Ellipsoidal Metal Particles with Nonlinear Dielectric Functions

In this section, we consider the local field in metal ellipsoidal particles while accounting for the nonlinear part of $\varepsilon(\omega, \mathbf{E})$ in (1). It may be found with the help of Eq. (4). But the direct usage of this equation is inconvenient, since it contains complex coefficients. It is better to rewrite it with respect to $|\mathbf{E}|^2$. Introducing the definitions $X = |\chi| |\mathbf{E}|^2$ and $Y = \left| \frac{\varepsilon_h}{L} \right|^2 |\chi| |E_h|^2$, we obtain the cubic equation for X ,

$$X^3 + aX^2 + bX = Y, \quad (8)$$

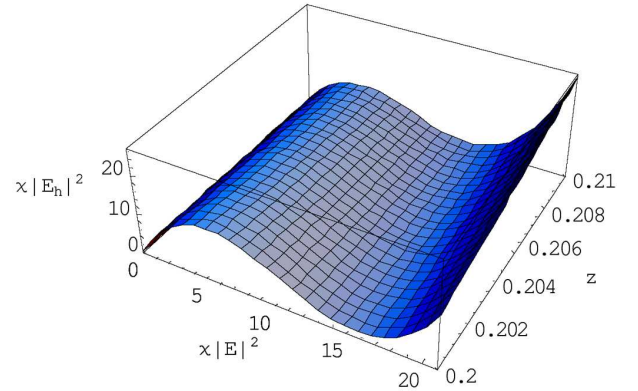


Fig. 3. Applied field $\chi|E_h|^2$ versus the local field $\chi|E|^2$ and the frequency z at $L = 0.33$ with the rest parameters as in Fig. 1

where

$$a = 2 \left(\frac{\tilde{\varepsilon}' \chi' + \tilde{\varepsilon}'' \chi''}{|\chi|} \right), \quad b = |\tilde{\varepsilon}|^2.$$

Relation (8) determines a dependence of the “local field” X on the “applied field” Y , dimensionless frequency z , depolarization factor L , and other parameters of the system. The enhancement factor with account of the above-specified quantities is given by a simple relation

$$|F|^2 = \left| \frac{\varepsilon_h}{L} \right|^2 \frac{X}{Y}. \quad (9)$$

Further, we are interested only in the real and positive roots of the cubic equation (8). If this equation has one real positive root, then the local field in the inclusion is a single-valued function of the applied field. If Eq. (8) has three positive roots, then the local field is not a single-valued function of the applied field, and the system becomes unstable. This situation is called the induced optical bistability (IOB).

To obtain the general picture of the connection between the applied field, local field, and the frequency, we decided to present a 3D graph involving these quantities. The 3D graph depicted in Fig. 3 is obtained with the help of (8) and shows the most interesting region of these parameters (bistability), when three different values of the local field correspond to one value of the applied field.

While analyzing the bistability phenomena in the system, it is more convenient to consider the dependence of a local field on the applied field. Figure 4 shows such dependences for different depolarization factors obtained with the help of (8) at $z = 0.2$. One can see that the bistability region (three different values of $\chi|E|^2$ for one value of $\chi|E_h|^2$) widens, as the depolarization factor L increases. Unfortunately, Fig. 4 is obtained for

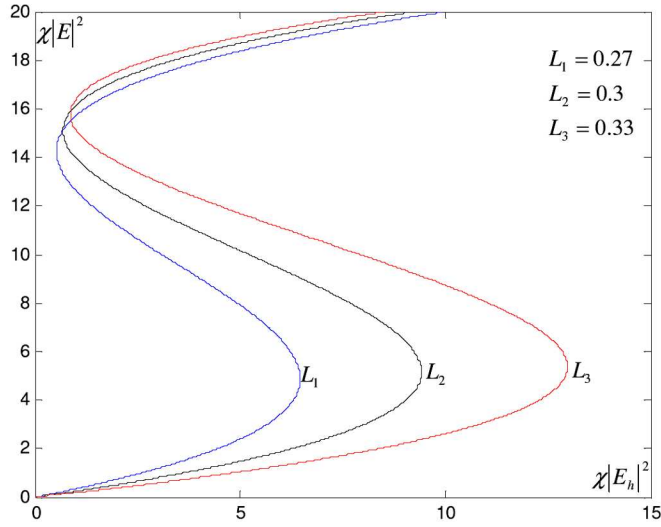


Fig. 4. Local field $\chi|E|^2$ versus the applied field $\chi|E_h|^2$ at the frequency $z = 0.2$ for different L ; the rest parameters as in Fig. 1

a fixed frequency of the incident electromagnetic wave. The bistability domain in the plane $(z, \chi|\mathbf{E}_h|^2)$ can be specified from an analysis of the roots of the cubic equation (8).

Two ways of finding the root location of a cubic equation are described in Appendices A and B. Now, we analyze the roots of (8) and find the IOB domain in the plane $(z, \chi|\mathbf{E}_h|^2)$. Equation (8) has three real positive roots provided conditions (47) are satisfied. In the case under consideration, these conditions may be written in the form

$$a \leq -\sqrt{3b}, \quad a < 0, \quad -\frac{2}{9} \left[DX_2 + \frac{ab}{2} \right] < Y < -\frac{2}{9} \left[DX_1 + \frac{ab}{2} \right], \quad (10)$$

where

$$X_{1,2} = \frac{-a \mp \sqrt{D}}{3}, \quad D = a^2 - 3b. \quad (11)$$

According to Appendix A, $X_{1,2}$ are the positions of extremum points of the function presented by the left-hand side of (8). They are determined from the equation $3X^2 + 2aX + b = 0$.

It is easy to show that

$$D = \frac{[(\tilde{\varepsilon}'\chi' + \tilde{\varepsilon}''\chi'')^2 - 3(\tilde{\varepsilon}''\chi' + \tilde{\varepsilon}'\chi'')^2]}{|\chi|^2}. \quad (12)$$

It follows from (10) and (11) that IOB emerges provided that $\tilde{\varepsilon}'' > 0$, $\chi'' > 0$, and quantities χ' and $\tilde{\varepsilon}'$ have

different signs. Below, we carry out a detailed analysis of the case $\tilde{\varepsilon}' < 0$, $\chi' > 0$.

As an aside, it is possible to find the IOB frequency domain analytically in the case $x_1 = x_2$. The general case requires numerical calculations.

Let us consider the non-absorbing host medium ($\varepsilon_h'' = 0$) containing the metal inclusion with the non-absorbing nonlinear part of the dielectric function ($\chi' > 0$, $\chi'' = 0$). In this case, Eq. (8) takes the form

$$X^3 + 2\tilde{\varepsilon}'X^2 + |\tilde{\varepsilon}|^2X = Y, \quad (13)$$

where

$$\tilde{\varepsilon}'(z) = \frac{1}{z_s^2} - \frac{1}{z^2 + \gamma^2}, \quad (14)$$

$$\tilde{\varepsilon}''(z) = \varepsilon_\infty''(z) + \frac{\gamma}{z(z^2 + \gamma^2)}. \quad (15)$$

The dimensionless frequencies z , z_s , γ were specified in (7). The first inequality (10) implies that IOB exists at frequencies z that satisfy the inequality

$$z^3\beta - z(z_s^2 - \gamma^2\beta) + \sqrt{3}z_s^2\gamma \leq 0, \quad (16)$$

where $\beta = (1 + \sqrt{3}z_s^2\varepsilon_\infty'') > 0$. To solve inequality (16), we consider the cubic equation

$$z^3\beta - z(z_s^2 - \gamma^2\beta) + \sqrt{3}z_s^2\gamma = 0. \quad (17)$$

This equation at $z_s^2 - \gamma^2\beta > 0$ has two positive roots (z_2, z_3) and one negative root, provided that its discriminant Q is negative, and the coefficients of this equation are positive and close to the surface plasmon frequency $z^2 < z_s^2 - \gamma^2$ (see Appendix B). The boundary frequencies of the IOB domain can be found from the cubic equation (17). Differentiating the function, which is the left-hand side of (17) with respect to z , we find the extremum points $\pm\sqrt{(z_s^2 - \gamma^2\beta)/(3\beta)}$. Substituting them into (17), we obtain the inequality

$$-(z_s^2 - \gamma^2\beta)^3 + \frac{81}{4}z_s^4\gamma^2 \leq 0. \quad (18)$$

As follows from Appendix A, at points z_2 and z_3 , $a^2 - 3b = 0$ ($a = 2\tilde{\varepsilon}'$, $b = |\tilde{\varepsilon}|^2$). The critical magnitudes of the electric fields at these points are (49)

$$(x_c)_{2,3} = -\frac{2}{3} \left(\frac{1}{z_s^2} - \frac{1}{z_{2,3}^2 + \gamma^2} \right), \quad (y_c)_{2,3} = (x_c)_{2,3}^3. \quad (19)$$

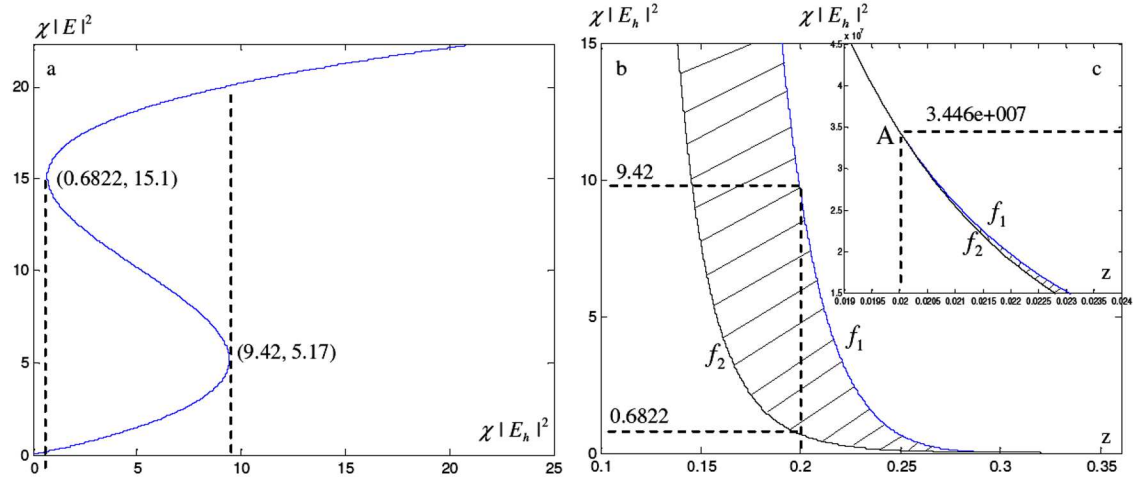


Fig. 5. Ellipsoidal silver particle with the parameters $L = 0.3$, $\varepsilon'_h = 2.25$, $\varepsilon''_h = 0$, $\varepsilon'_\infty = 4.5$, $\varepsilon''_\infty = 0.16$, $\gamma = 1.15 \times 10^{-2}$. (a) The IOB for a local field $\chi|E|^2$ versus the applied field $\chi|E_h|^2$ at the frequency $z = 0.2$. The IOB domain in the plane $(z, \chi|E_h|^2)$ (shaded area). (b) High-frequency limit part of the IOB domain. (c) Low-frequency limit part of the IOB domain

At $Q = 0$, $z_1 = z_2 = z_c$, the critical magnitude of the field y_c coincides, according to (19), with a minimum value of the external electric field when the bistability emerges in the system. Therefore, in the case under consideration, IOB in the system emerges in the frequency band

$$z_2 \leq z \leq z_3. \quad (20)$$

The range of applied fields is again specified by the second inequality (10). Roots $z_2 > 0$, $z_3 > 0$ can be found from (18) which has three real roots. Inequality (18) at fixed β and z_s and at $\frac{\gamma^2 \beta}{z_s^2} \ll 1$ allows one to obtain the critical γ_c :

$$\gamma_c = \frac{2}{9} z_s \left(1 - \frac{4}{81} \beta \right)^{3/2}. \quad (21)$$

If the collision damping $\gamma > \gamma_c$, then IOB disappears. We may suggest that any increase in the damping that exists in the inclusion makes the conditions for the IOB emergence more restrictive. A minimum critical value of the external electric field for the IOB emergence can be found from (19). It is given by the relation

$$|\chi| \cdot |\mathbf{E}_h|_c^2 = \left(\frac{L}{\varepsilon_h} \right)^2 \cdot \left(\frac{1}{z_3^2 + \gamma^2} - \frac{1}{z_s^2} \right)^3, \quad (22)$$

where z_3 is the larger of the roots z_2 and z_3 of Eq. (17). If ε''_∞ and γ tend to zero, the critical electric field tends to zero as well.

The curves $f_{1,2}$ restricting the IOB domain in the plane $(z, \chi|\mathbf{E}_h|^2)$ can be obtained from the equations

$$f_i = -(2/9)[Dx_i + ab/2](L/\varepsilon_h)^2, \quad i = 1, 2. \quad (23)$$

Figure 5 depicts the IOB domain (shaded area) in the plane $(z, \chi|\mathbf{E}_h|^2)$ for an ellipsoidal silver particle. The boundaries of the IOB domain (curves f_1 and f_2) have been calculated with the help of formula (23).

Below, we present the IOB domain for the curve $L_2 = 0.3$. It corresponds to the lowest applied and local fields as compared with those for the bistability domains with $L_1 = 0.27$ and $L_3 = 0.33$. The bistability domains for the polarization factors corresponding to L_1 and L_3 have the same style as depicted in Fig. 5. But the bistability domain is narrower for L_1 and is wider for L_3 than for L_2 in accordance with the range of applied fields.

The limiting values of the incident electric field are shown in Fig. 5 by a dashed line at $\omega = 0.2\omega_p$. Figure 5,b shows the bistability domain near a point z_2 (the smaller root of Eq. (17)). The entire bistability domain looks like an area enclosed by a hysteresis-type curve. Its upper part gets narrowing with increase in the external field. We would like to note that IOB in a spherical metal particles has been studied in many papers and in [1], particularly.

We would like to note that the upper end of the bistability domain in Fig. 5,c, point A, corresponds to $z = 0.02$, $\gamma = 0.0115$ and considerably high applied fields. We also have calculated $\chi|E|^2$ versus $\chi|E_h|^2$ for

different γ with the same rest parameters as in Fig. 1. The results show that the IOB practically disappears at $\gamma = 3 \times 0.0115$.

4. Bistability in Coated Spherical Particles

We now consider a spherical dielectric particle (the core) of radius r_1 covered by a metal shell of radius r_2 . Let the core be a nonlinear dielectric of the Kerr type with the nonlinear dielectric function (DF)

$$\varepsilon_1 = \varepsilon_{10} + \chi |\mathbf{E}|^2, \quad (24)$$

where ε_{10} is the linear part of DF, χ is the nonlinear Kerr coefficient that depends, in a general case, on the frequency of the electromagnetic field, and \mathbf{E} is the amplitude of the local field in the core. The dielectric function of the metal shell will again be of the Drude type [9]

$$\varepsilon_2 = \varepsilon_\infty - \frac{1}{z(z + i\gamma)}, \quad (25)$$

where z and γ are given by (7). In the long-wavelength limit (the electrostatic approximation), the electric field within the inclusion or the local field can be found from the relation (3) with the enhancement factor F given by the expression

$$F = \frac{3}{p} \frac{\varepsilon_2 \varepsilon_h}{\Delta},$$

$$\Delta = \varepsilon_2^2 + [(3/2p - 1)\varepsilon_1 + (3/p - 1)\varepsilon_h]\varepsilon_2 + \varepsilon_1 \varepsilon_h. \quad (26)$$

Here, $p = 1 - r_1^3/r_2^3$ is the metal fraction in the inclusion particle. One can easily see that (26) for a completely metallic particle ($p = 1$) gives the same enhancement factor as (3) for a spherical metallic particle ($L = 1/3$).

It is clear that one may obtain a considerable increase in the local electric field provided that the denominator of (26) tends to zero. This condition can be realized by tuning the parameters that comprise Δ .

In the limit $\gamma \ll 1$ (the collision frequency of electrons is small as compared with the plasma frequency), the imaginary part of (25) can be neglected. In this case, the "resonance" condition ($\Delta = 0$) reduces to a quadratic equation in ε_2 with the roots

$$\varepsilon_{2\pm} = (-s \pm \sqrt{s^2 - 4\varepsilon_1 \varepsilon_h})/2,$$

$$s = (3/2p - 1)\varepsilon_1 + (3/p - 1)\varepsilon_h. \quad (27)$$

We note that, in our case, $s < 0$ and $\varepsilon_{2\pm} < 0$ always. Moreover, $\varepsilon_{2-} < \varepsilon_{2+}$. In the limiting case of a small metal fraction, $p \ll 1$, expressions (27) may be simplified to

$$\varepsilon_{2-} = -\frac{3(\varepsilon_1 + 2\varepsilon_h)}{2p}, \quad \varepsilon_{2+} = -\frac{2\varepsilon_1 \varepsilon_h}{3(\varepsilon_1 + 2\varepsilon_h)} p,$$

$$p \ll 1. \quad (28)$$

Since $\varepsilon_{2\pm} < 0$, the realization of a local field enhancement requires $\text{Re}\varepsilon_2(\omega) < 0$ as well. One can see from (25) that it takes place at frequencies $\omega < \omega_0 = \omega_p/\sqrt{\varepsilon_\infty}$ (we assumed that $\omega_0 \gg \nu$). The frequency ω_0 corresponds to the bulk plasmon frequency. It also follows from (3), (26), and (27) that a maximum enhancement of the local field occurs when the frequency of an electromagnetic wave approaches

$$\omega_{s\pm} = \frac{\omega_p}{\sqrt{\varepsilon_\infty - \varepsilon_{2\pm}}}. \quad (29)$$

For example, at $p \ll 1$, when the metal fraction of an inclusion is comparatively small, $\omega_{s-} \rightarrow 0$, $\omega_{s+} \rightarrow \omega_0$. Here, we would like to note that the polarizability of a two-layer spherical inclusion may be presented in the form [8]

$$\alpha = 4\pi r_2^3 \frac{\bar{\varepsilon} - \varepsilon_h}{\bar{\varepsilon} + 2\varepsilon_h}, \quad (30)$$

where $\bar{\varepsilon}$ is the effective dielectric function of the individual two-layer inclusion in the dipole approximation and given by the relation

$$\bar{\varepsilon} = \varepsilon_2 \frac{\varepsilon_1(3/p - 2) + 2\varepsilon_2}{\varepsilon_1 + \varepsilon_2(3/p - 1)}. \quad (31)$$

Combining (30) and (31), one may easily show that the enhancement factor (26) and the polarizability coefficient (30) have the same denominator Δ (26). This means that α increases considerably when the frequency ω approaches one of the frequencies (29). At the same time, the absorption of radiation by a particle increases due to an increase in the polarization.

The local field enhancement within a coated spherical particle means that the nonlinear term in (24) must be taken into account. Therefore, the enhancement factor F (26) itself depends on the local field \mathbf{E} , and, in the general case, relation (3) turns out to be the equation for the local field as a function of the applied field \mathbf{E}_h . Acting in the same manner as in Section 2 by deducing (8), we again obtain the cubic equation for the local field in the particle

$$X^3 + a_1 X^2 + b_1 X = \eta Y,$$

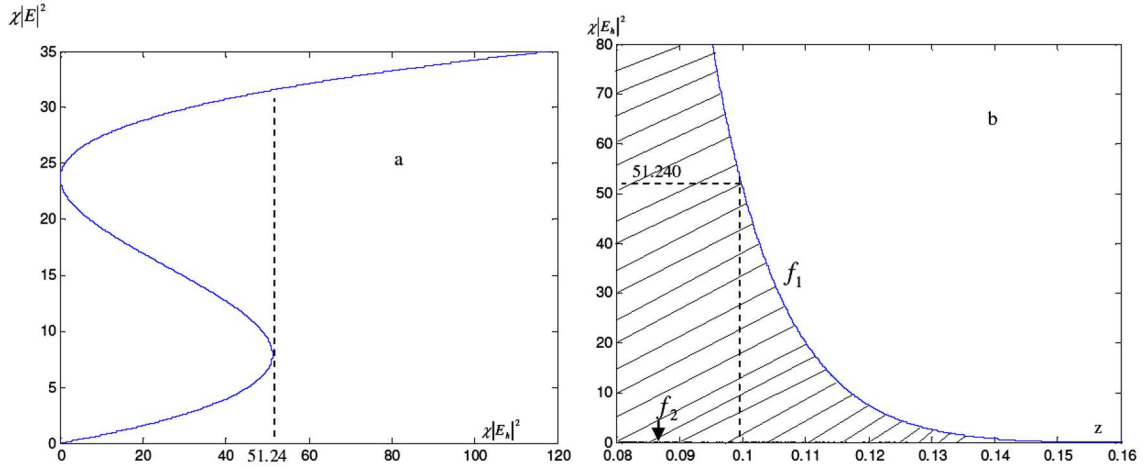


Fig. 6. IOB in a coated spherical particle: $\varepsilon_{10} = 6.00$, $\varepsilon_{\infty} = 4.5$, $\varepsilon_h = 2.25$, $p = 0.4$, $\gamma = 0$. a) The local field $\chi|E|^2$ versus the applied field $\chi|E_h|^2$ at $z = 0.1$, b) IOB domain (shaded area) in the plane $(z, \chi|E_h|^2)$. The curves f_1 and $f_2 = 0$ are calculated with the help of (33)

$$a_1 = 2\text{Re}\left(\frac{\Delta_0}{\delta}\right), b_1 = \left|\frac{\Delta_0}{\delta}\right|^2,$$

$$\Delta_0 = (\varepsilon_2)^2 + \varepsilon_2 \left[\varepsilon_{10} \left(\frac{3}{2p} - 1 \right) + \left(\frac{3}{p} - 1 \right) \varepsilon_h \right] + \varepsilon_{10} \varepsilon_h,$$

$$\eta = \frac{9}{p^2} \left| \frac{\varepsilon_2 \varepsilon_h}{\delta} \right|^2, \delta = \varepsilon_h + \frac{\varepsilon_2}{2p} (3 - 2p). \quad (32)$$

Here, Δ_0 is obtained from (26) by the substitution $\varepsilon_1 \rightarrow \varepsilon_{10}$.

This cubic equation has real coefficients and may have one real positive root or three real positive roots depending on its parameters (Appendices A and B). Therefore, in some domain of frequencies and amplitudes of the incident electromagnetic wave, IOB may occur. The domain of instability can be specified in the same manner, as it was done in the previous section.

Here, we briefly discuss the final results. The IOB in a coated spherical particle emerges under the following conditions (in notations of (32)):

$$a_1 \leq -\sqrt{3b_1}, \quad a_1 < 0,$$

$$-\frac{2}{9} \left[D_1 X_2 + \frac{a_1 b_1}{2} \right] < Y < -\frac{2}{9} \left[D_1 X_1 + \frac{a_1 b_1}{2} \right]. \quad (33)$$

The boundaries of the IOB domain are specified by the curves

$$f(X_i) = -\frac{2}{9\eta} \left[D_1 X_i + \frac{a_1 b_1}{2} \right], \quad i = 1, 2, \quad (34)$$

$$X_{1,2} \text{ are the extremum points of } f(X) = X^3 + a_1 X^2 + b_1 X,$$

$$D_1 = a_1^2 - 3b_1.$$

Since $\varepsilon_{10} > 0$ and $\varepsilon_h > 0$ in our case, there is no IOB in the frequency region where $\text{Re}\varepsilon_2(\omega) > 0$. The second inequality of (33) determines the range of the applied field where IOB appears.

Now we again return to a simplified version of the theory, when the imaginary parts of ε_1 and ε_2 can be neglected. In this situation, the first condition for the IOB emergence reduces to

$$\Delta_0 \delta < 0. \quad (35)$$

This inequality can be presented in the form

$$(\omega - \omega_{S-}^{(0)})(\omega - \omega_{S+}^{(0)})(\omega - \omega_{S1}) < 0, \quad (36)$$

where the frequencies $\omega_S^{(0)}$ are given by (29) with ε_1 substituted by ε_{10} ,

$$\omega_{S1} = \frac{\omega_p}{\sqrt{\varepsilon_{\infty} - \varepsilon_0}}, \quad \varepsilon_0 = \frac{2p}{3 - 2p}. \quad (37)$$

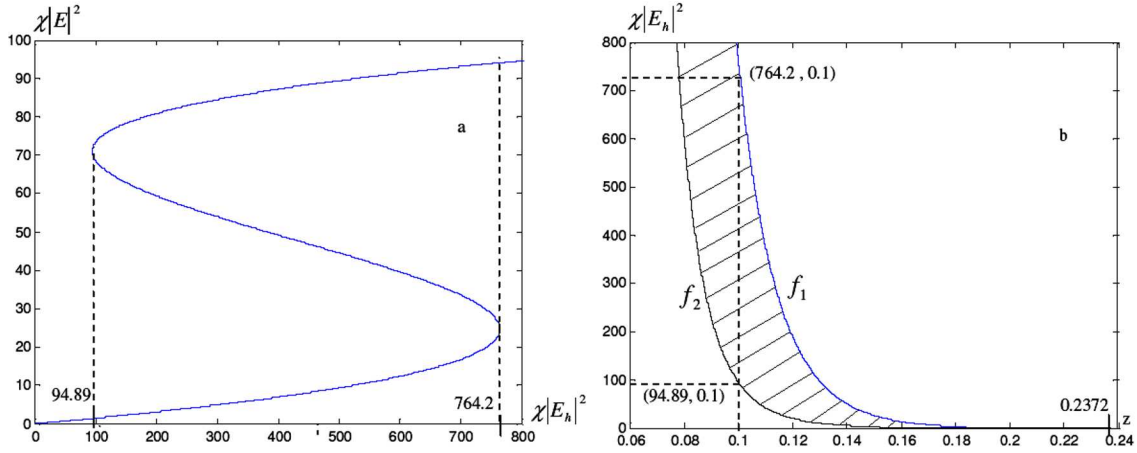


Fig. 7. IOB in a spherical particle with a silver cover: $\varepsilon_{10} = 6.00$, $\varepsilon_{\infty} = 4.5$, $\varepsilon_h = 2.25$, $p = 0.7$, $\gamma = 0.0115$. a) The local field $\chi|E|^2$ versus the applied field $\chi|E_h|^2$ at $z = 0.1$, b) IOB domain (shaded area) in the plane $(z, \chi|E_h|^2)$

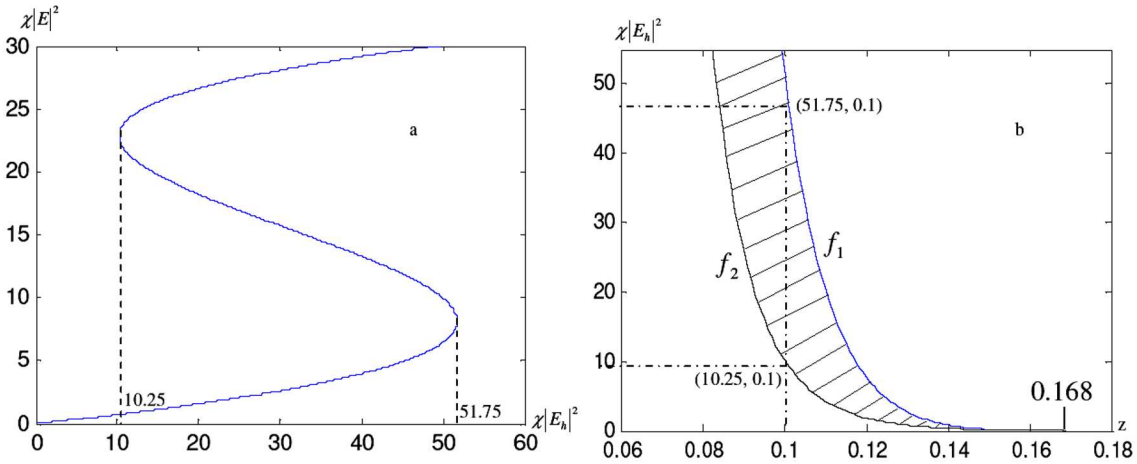


Fig. 8. IOB in a spherical particle with a silver cover: $\varepsilon_{10} = 6.00$, $\varepsilon_{\infty} = 4.5$, $\varepsilon_h = 2.25$, $p = 0.4$, $\gamma = 0.0115$. a) The local field $\chi|E|^2$ versus the applied field $\chi|E_h|^2$ at $z = 0.1$, b) IOB domain (shaded area) in the plane $(z, \chi|E_h|^2)$

It is clear that $\omega_{S-}^{(0)} < \omega_{S+}^{(0)} < \omega_{S1}^{(0)}$. In addition, in this case,

$$x_1 = -\frac{\Delta_0}{\delta}, \quad x_2 = -\frac{3\Delta_0}{\delta}, \quad (38)$$

$$f(x_1) = -\frac{4}{27} \left(\frac{\Delta_0}{\delta}\right)^3, \quad f(x_2) = 0.$$

Summing up these results, we can state that IOB emerges in a two-layer spherical particle with the Kerr-type nonlinear dielectric core (DF (24)) covered with a metal shell with no decay (the Drude-type dielectric function (25) with zero imaginary part) in the following two frequency bands:

$$0 < \omega < \omega_{S-}^{(0)} \quad \text{and} \quad \omega_{S+}^{(0)} < \omega < \omega_{S1}^{(0)}. \quad (39)$$

IOB does not exist if the external field exceeds the critical value

$$E_c = \frac{4p\varepsilon_h}{27|\varepsilon_2|} \sqrt{\frac{|\Delta_0|^3}{3\chi\delta}}. \quad (40)$$

Below, we illustrate typical dependences of the local field on the applied field (Fig. 7,a and Fig. 8,a) that are obtained from the solution of the cubic equation (32) and IOB domains (Fig. 7,b and Fig. 8,b) from the bistability conditions (relation (33)). We have calculated the IOB domains for different p in the range 1–0.25 at $\gamma = 0.0115$. The results show that the IOB domain decreases with the metallic fraction. In particular, if γ increases three times, the

IOB completely disappears in the elliptic metal particles.

5. Conclusion

We now recount the main theoretical conclusions that follow from this study. In Section 2, we considered the enhancement of the local field in a small ellipsoidal metal particle in the linear approximation. The enhancement factor is largest if the frequency of the incident light coincides with the surface plasmon frequency of a particle ω_s . This value depends, in turn, on the depolarization factor L and can have a maximum at definite L (Fig. 1). In Section 3, we studied the induced optical bistability domain (IOB) for ellipsoidal metal particles with regard for the nonlinear part of its dielectric function. In the intensity-frequency plane of the incident electromagnetic wave, this domain is the area restricted by a hysteresis-like curve. The upper part of the domain area becomes narrower with increase in the amplitude of the electromagnetic wave. IOB takes place in a range of frequencies near the surface plasmons of the inclusion. The critical fields of beginning and disappearance of IOB are determined. We note that the entire domain of IOB had not been studied in the literature prior to this study. Section 4 was devoted to a study of the electrodynamic properties of small spherical particles with a nonlinear dielectric and covered by the metal shell. We have found that IOB in inclusions of this type can emerge in two-frequency bands (the range of a surface plasmon of the particle). The metal covering of the nonlinear dielectric makes the enhancement of a local field easier to the required level for the IOB emergence than without the metal covering. The dependences of the local field on the applied electric field have been calculated for particular systems by solving a cubic equation of the type (8). We may state that increasing the electron damping in the systems under study suppresses IOB according to relation (18).

Finally, one more interesting fact should be noted. We determined the local field by solving the corresponding cubic equation for other systems than those considered in this paper. In particular, a two-layer plane structure of a metal and a nonlinear dielectric, a sphere with a nonlinear dielectric in a metal host matrix, and a two-layer ellipsoid with a nonlinear dielectric and a metal covering in the case where the external electric field is parallel to one of its axes. At the same time, in the case of a two-layer ellipsoid at an arbitrary orientation of the external electric field, the order of this equation becomes

higher. Changes in the order of equations may produce more complex pictures of IOB in these systems.

APPENDIX A

Here, we consider the location and the motion of the roots to the cubic equation

$$x^3 + ax^2 + bx + c = 0 \quad (41)$$

in the complex plane $x = x' + ix''$ depending on variations of the parameter c . In Eq. (41), the parameters a , b , and c are real. In our case, $b \geq 0$, $c = -y$ ($y > 0$), and a may be both positive and negative. In this paper, we are concerned with the conditions imposed on the coefficients a , b , and y when this equation has three (or one) real positive roots. It is known that the answer to this question is given by the Routh–Hurwitz theorem [10]. The location of the roots of (41) that depend on its coefficients which follows from the Routh–Hurwitz theorem is given in the table of Appendix B. In particular, (41) has three real positive roots provided that

$$D \leq 0, \quad b > 0, \quad y > 0, \quad ab + y > 0, \quad (42)$$

where D is a discriminant of Eq. (41)

$$D = \left(\frac{H}{3}\right)^3 + \left(\frac{q}{2}\right)^2, \quad H = \frac{a^3}{3} + b, \quad q = 2\left(\frac{a}{3}\right)^3 - \frac{ab}{3} - y. \quad (43)$$

One can see that these conditions are rather complex for an analysis. Here, we use a simpler way [5]. From the graphical analysis of Eq. (41), one may see that it has three (or one) real roots if the extremum points (if they exist) of the function

$$y = x^3 + ax^2 + bx \quad (44)$$

are positive

$$x_1 > 0, \quad x_2 > 0, \quad (45)$$

and any positive y_0 lies in the interval

$$y(x_2) \leq y_0 \leq y(x_1), \quad (46)$$

where $x_1 \leq x_2$. For (41), these conditions can be written in the form

$$\begin{cases} a < -\sqrt{3b}, \\ -\frac{2}{9} \left[(a^2 - 3b)x_2 + \frac{ab}{2} \right] < y_0 < -\frac{2}{9} \left[(a^2 - 3b)x_1 + \frac{ab}{2} \right]. \end{cases} \quad (47)$$

Therefore, the intervals where the cubic equation (41) has three real positive roots are given by the following expressions:

$$\begin{aligned} \Delta(x) &= x_2 - x_1 = \frac{2}{3}(a^2 - 3b)^{1/2}, \\ \Delta(y) &= y(x_1) - y(x_2) = \frac{4}{27}(a^2 - 3b)^{3/2}. \end{aligned} \quad (48)$$

We note that, at $a^2 - 3b = 0$, $x_2 = x_1 = x_c$ and $y_2 = y_1 = y_c$. Then, at the same time,

$$x_c = -\frac{a}{3}, \quad y_c = -\frac{a^3}{27}. \quad (49)$$

The magnitudes x_c and y_c specify the critical values of x and y when three real positive roots appear in Eq. (41).

Range of parameters	Location of roots on the complex plane
$x^3+ax^2+bx+c=0, Q=(H/3)^3+(G/2)^2 < 0, H=-a^2/3+b, G=2(a/3)^3-ab/3+c$. In this case, all roots are real	
$ab-c < 0, c < 0, b > 0$	
$ab-c > 0, c > 0, b > 0$	
$ab-c < 0, c > 0, b > 0$ or $c > 0, b \le 0$	
$ab-c > 0, c < 0, b > 0$ or $c < 0, b \le 0$	
$x^3+ax^2+bx+c=0, Q=(H/3)^3+(G/2)^2 > 0, H=-a^2/3+b, G=2(a/3)^3-ab/3+c$. In this case, one root is real and two roots are complex conjugate	
$ab-c < 0, c < 0, b > 0$	
$ab-c > 0, c > 0, b > 0$	
$ab-c < 0, c > 0, b > 0$ or $c > 0, b \le 0$	
$ab-c > 0, c < 0, b > 0$ or $c < 0, b \le 0$	

APPENDIX B

Here, we give the table of an arrangement of roots of the cubic equation depending on its parameters.

1. R.W. Boyd, *Nonlinear Optics* (Academic Press, New York, 1992).
2. A. Szöke, V. Daneu, J. Goldhar, and N.A. Kurnit, *Appl. Phys. Lett.* **15**, 376 (1969).
3. H.M. Gibbs, S.L. McCall, and T.N.C. Venkatesan, *Phys. Rev. Lett.* **36**, 113 (1976).
4. K.M. Leung, *Phys. Rev. A* **33**, 2461 (1986).
5. N. Kalyaniwalla, J.W. Haus, R. Inguva, and M.H. Birnboim, *Phys. Rev. A* **42**, 5613 (1990).

6. R. Neuendorf, M. Quentin, and U. Kreibig, *J. Chem. Phys.* **104**, 6348 (1996).
7. G. Jungk, *Phys. Stat. Sol. (b)* **146**, 335 (1988).
8. O. Levy and D.J. Bergman, *Physica A* **207**, 157 (1994).
9. J.W. Haus, N. Kalyaniwalla, R. Inguva, and C.M. Bowden, *J. Opt. Soc. Am.* **61**, 797 (1989).
10. M.A. Palenberg and B.U. Felderhof, *Phys. Rev. B* **55**, 10326 (1997).
11. L.G. Grechko, O.A. Davidova, V.N. Mal'nev, and K.W. Whites, in *Chemistry, Physics, and Technology of Surfaces, Issues 4-6* (Institute of Surface Chemistry of the NAS of Ukraine, Kyiv, 2001), pp. 168-177.
12. Min Xiao and Shaozheng Jin, *Phys. Rev. A* **45**, 483 (1992).
13. Lei Gao, Liping Gu, and Zhenya Li, *Phys. Rev. E* **68**, 066601 (2003).
14. Wei Zhang, Yuanyuan Chen, Jielong Shi, and Qi Wang, *Phys. Rev. E* **81**, 046603 (2010).
15. C.F. Bohren and D.R. Huffman, *Absorption and Scattering of Light by Small Particles* (Wiley, New York, 1983).
16. G.A. Korn and T.M. Korn, *Mathematical Handbook for Scientists and Engineers* (McGraw-Hill, New York, 1968).

Received 24.01.11

ІНДУКОВАНА ОПТИЧНА ВІСТАБІЛЬНІСТЬ У МАЛЕНЬКИХ МЕТАЛЕВИХ І ПОКРИТИХ МЕТАЛОМ ЧАСТИНКАХ З НЕЛІНІЙНОЮ ДІЕЛЕКТРИЧНОЮ ФУНКЦІЄЮ

О.А. Бурій, Л.Г. Гречко, В.М. Мальнев, С. Шевамаре

Резюме

Виконано теоретичне та чисельне дослідження резонансного збільшення амплітуди електромагнітного випромінювання в маленьких металевих еліпсоїдальних частинках та сферичних діелектричних частинках з металічною оболонкою. При наближенні частоти випромінювання до частоти поверхневих плазмонів металу має місце суттєве підвищення локального електричного поля в середині частинки. При великих (лазерних) напруженостях полів необхідно враховувати нелінійну частину діелектричної функції в металі та діелектрику. Це приводить до виникнення індукованої оптичної бістабільності (ІОБ), коли одному значенню амплітуди падаючого поля відповідає три значення локального поля. Дослідження ІОБ виконано для випадку, коли довжина хвилі випромінювання набагато більша, ніж типові розміри частинок. Визначено інтервали зовнішніх полів ті діапазони частот ІОБ. Досліджено зменшення області ІОБ та збільшення критичних полів з ростом затухання плазмових коливань. Результати чисельних розрахунків представлено графічно.